

Supercritical-subcritical correspondence, asymmetric effects and antisymmetric corrections near a critical point

Xinyang Li¹ and Yuliang Jin^{2,3,4,*}

¹*Peng Huanwu Collaborative Center for Research and Education, Beihang University, Beijing 100191, China*

²*Institute of Theoretical Physics, Chinese Academy of Sciences, Beijing 100190, China*

³*School of Physical Sciences, University of Chinese Academy of Sciences, Beijing 100049, China*

⁴*Wenzhou Institute, University of Chinese Academy of Sciences, Wenzhou, Zhejiang 325000, China*

(Dated: December 10, 2025)

The second-order phase transitions in the Ising model and liquid-gas systems share a universality class and critical exponents, despite the absence of Z_2 symmetry in the liquid-gas Hamiltonian. This discrepancy highlights a central puzzle in critical phenomena: what is the influence of asymmetry on scaling laws? For over a century, this question has been explored through examining violations of the empirical “rectilinear diameter law” for the subcritical coexistence curve, where asymmetry could generate singular corrections. Here, we extend this investigation to the supercritical regime. We propose a supercritical-subcritical correspondence, drawing a formal analogy between the subcritical coexistence curve and recently defined supercritical boundary lines (L^\pm lines). Our theory predicts that the linear mixing of physical fields - a hallmark of asymmetric systems - produces universal scaling corrections, with antisymmetric coefficients, in these supercritical loci. We verify these predictions using liquid-gas data from the NIST database and a model liquid-liquid transition. Furthermore, we demonstrate that the same asymmetric scaling framework governs the behavior of higher-order cumulants in the order parameter distribution.

Introduction. The notion of universality is well established for critical phenomena – systems belonging to the same universality class share the same critical exponents, independent of microscopic details. However, such systems do not need to present the same symmetry. A paradigmatic example is the comparison between the ferromagnetic-paramagnetic phase transition in the Ising model and the liquid-gas critical point, both of which belong to the Ising universality class [1]. The Ising Hamiltonian has an obvious Z_2 symmetry because the energy is invariant if all spins are flipped. In the case of the liquid-gas critical point, the elementary lattice gas model enjoys the same Z_2 symmetry – termed a “particle-hole symmetry” – since it can be directly mapped to the Ising model [2]. However, such a symmetry disappears if the particles are allowed to move continuously in the space, or the Hamiltonian is redefined to be asymmetric in the lattice gas model [3]. In general, realistic liquid-gas systems conform the Ising universal critical exponents without the Z_2 symmetry – for this reason, such systems are often called “asymmetric”. In fact, asymmetric systems are ubiquitous in the nature; most phase transitions (liquid-gas, liquid-liquid, etc.) in atomic and molecular systems are asymmetric.

According to the above definition, asymmetric models do not have the Z_2 symmetry in their Hamiltonians. This feature is naturally reflected in the equation of state (EOS). Without loss of generality, we consider the constant susceptibility lines in the external field-temperature phase diagram. In the magnetic field - temperature ($H - T$) phase diagram of the Ising model (Fig. 1A),

a typical contour line, along which the magnetic susceptibility $\chi = (\frac{\partial m}{\partial H})_T$ is a constant, is obviously symmetric with respect to the first-order transition coexistence line ($H = 0$). Contrarily, in the pressure - temperature ($P - T$) phase diagram of the liquid-gas system, a contour line with a constant compressibility $\kappa_T = (\frac{\partial \rho}{\partial P})_T$ does not have an apparent symmetry. In particular, such a line does not close a loop below the critical point. A key unresolved problem is the explicit role of asymmetry in the behavior of EOS near the critical point.

The asymmetric effects in the EOS have been indeed intensively discussed, with particular attention paid to the violation of the famous *law of rectilinear diameter* [4], which asserts a linear dependence of the mean liquid-gas density (“diameter” of the coexistence curve) $\rho_d = \frac{1}{2}(\rho_L + \rho_G)$ on $\Delta\hat{T} \equiv (T - T_c)/T_c$ near the critical temperature T_c ,

$$\rho_d = \rho_c + C|\Delta\hat{T}|, \quad (1)$$

where ρ_L and ρ_G are the liquid and gas densities at the same T , ρ_c the critical density, and C a system-dependent coefficient. Historically, this law played a very important role in determining the critical density [5]. The Ising model has $C = 0$, which is a special case of a linear relationship. For asymmetric systems, many theories have proposed a “singular diameter” [3, 6–13],

$$\rho_d = \rho_c + D_1|\Delta\hat{T}|^{2\beta} + D_2|\Delta\hat{T}|^{1-\alpha} + \dots, \quad (2)$$

where α and β are standard critical exponents. The expression shows $d\rho_d/dT$ diverging weakly near the critical point. However, experimental examinations on the asymptotic critical behavior of ρ_d are challenging [13–18]. An important reason is that the subcritical ($T < T_c$)

* yuliangjin@mail.itp.ac.cn

scaling regime for Eq. (2), whose size could be system-dependent, is too narrow to be detected in many systems.

All existing studies focus on studying the asymmetric effects on the EOS behavior in the subcritical regime ($T < T_c$). In this work, we switch our attention to the supercritical regime ($T > T_c$). There is no coexistence region in the phase diagram above T_c , and therefore one cannot define a diameter of the coexistence curve. However, an intriguing *supercritical-subcritical correspondence* is emerging, thanks to recently defined supercritical crossover lines L^\pm lines [19–23] (see Fig. 2 and their definitions below). These two lines serve as the boundary of the liquid-gas indistinguishable supercritical state, forming a “mirror image”, with respect to T_c , of the subcritical coexistence region. According to Fig. 2, both supercritical and coexistence regions represent transition states between liquid and gas states, although their properties are certainly different - below T_c two phases can coexist in equilibrium, while above T_c there is a single phase. Nevertheless, a recent study shows that the properties of the supercritical state (such as the radial distribution function and transport coefficients) evolve gradually from typical gas-like behavior at L^- line to liquid-like behavior at L^+ line [24]. These results inspire us to consider L^\pm lines as the supercritical counterpart of the subcritical coexistence curve, which is the starting point of this study.

Here we employ a linear scaling theory to examine the asymmetric effects, caused by linear mixing of fields, on the behavior the L^\pm lines near T_c . Interestingly, we find that the “supercritical diameter” $\rho_d^> = \frac{1}{2}(\rho^+ + \rho^-)$ violates the rectilinear law and follows Eq. (2), because the coefficients of correction terms are “antisymmetric”. This surprising coincidence with the behavior of the subcritical diameter ρ_d rationalizes our proposed subcritical-supercritical correspondence. Compared to the subcritical counterpart, the scaling of $\rho_d^>$ has a practical advantage: its scaling regime is significantly larger, making experimental verification easier. This advantage allows us to use the available data of supercritical fluids in the National Institute of Standards and Technology (NIST) database [25] to verify Eq. (2). The same asymmetric scaling is further validated by a model of liquid-liquid phase transition, and data extracted from higher-order cumulants of the order parameter distribution. Our results thus suggest that common scaling laws like Eq. (2) capture universally the asymmetric effects both below and above a critical point.

General results from a linear scaling theory. The thermodynamics near a critical point is described by a universal scaling function [26],

$$h_3(h_1, h_2) \simeq |h_2|^{2-\alpha} f(h_1/|h_2|^{\beta+\gamma}), \quad (3)$$

where h_1, h_2, h_3 are respectively the ordering field, thermal field (temperature), and singular part of the thermodynamic potential. The *linear scaling theory* [27, 28] parameterizes h_1 and h_2 with “polar” variables r and θ , $h_1 = ar^{\beta+\gamma}\theta(1-\theta^2)$ and $h_2 = r(1-b^2\theta^2)$, and assumes a

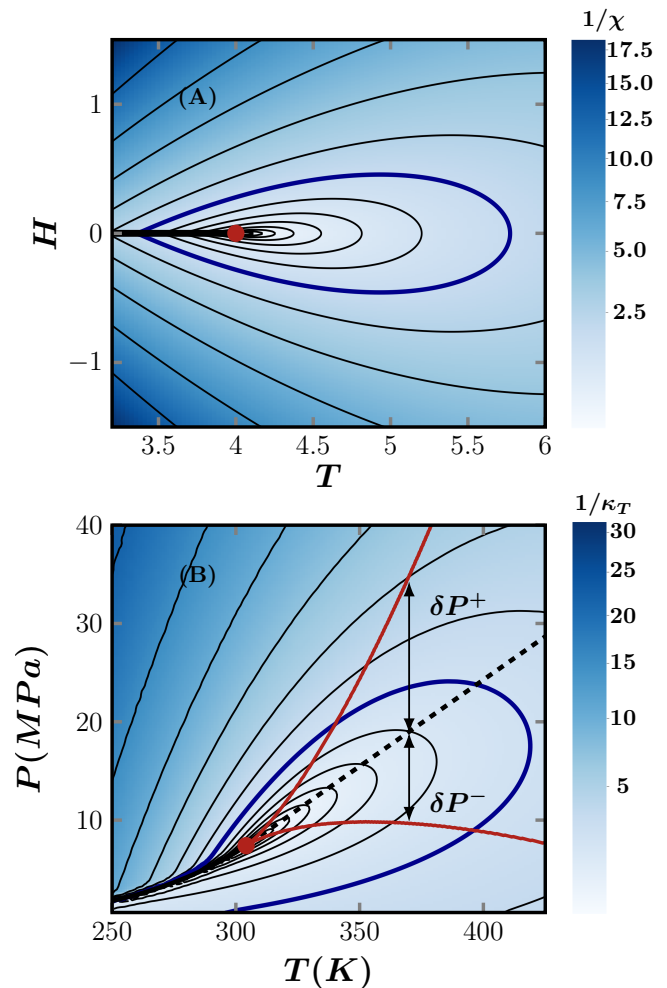


FIG. 1. **Phase diagrams and EOSs for symmetric and asymmetric systems.** (A) $H - T$ phase diagram of the 2D mean-field Ising model. (B) $P - T$ phase diagram of CO_2 , obtained from the NIST database [25]. The thick black line is the first-order transition (coexistence) line, and the red circle the critical point. The thin contour lines are constant order parameter EOSs, with one typical EOS highlighted by a thicker line. In (B), the dashed black line is the critical isochore ($\rho = \rho_c$), and the red lines are L^\pm lines [19].

linear function of the order parameter, $\phi_1 = \left(\frac{\partial h_3}{\partial h_1}\right)_{h_2} = kr^\beta\theta$, where a, k are system-dependent fitting parameters, and $b^2 = (\delta - 3)/(\delta - 1)(1 - 2\beta)$. Here γ and δ are standard critical exponents (see details in SM Sec. S1).

Following the idea of *complete scaling* [29, 30], we assume that the physical fields T, P and the chemical potential μ in an asymmetric liquid-gas system are linear mixing of h_1, h_2 and h_3 ,

$$\begin{aligned} h_1 &= \Delta\hat{\mu} - a_3 \tan\varphi\Delta\hat{T} + a_3\Delta\hat{P}, \\ h_2 &= \Delta\hat{T} + b_2\Delta\hat{\mu} + \tan\varphi\Delta\hat{P}, \\ h_3 &= \Delta\hat{P} - \Delta\hat{\mu} - \tan\varphi\Delta\hat{T}. \end{aligned} \quad (4)$$

Here $\Delta\hat{\mu} \equiv (\mu - \mu_c)/\mu_c$ and $\Delta\hat{P} \equiv (P - P_c)/(\rho_c k_B T_c)$.

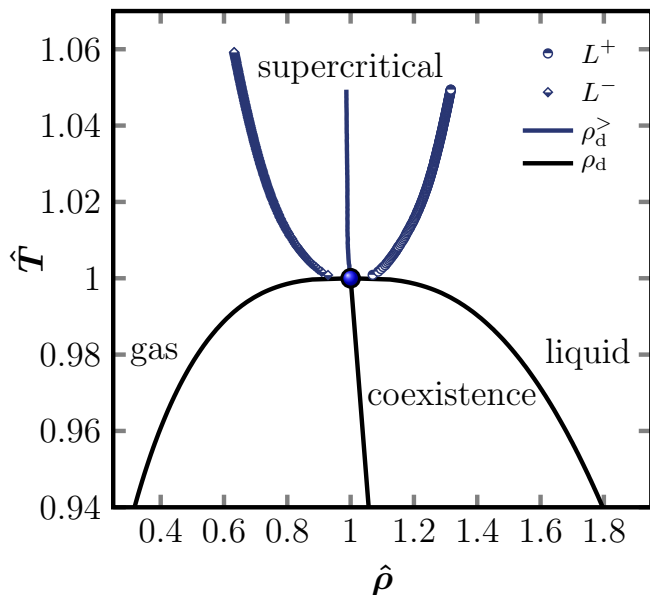


FIG. 2. **Supercritical-subcritical correspondence.** The following correspondence is visualized in the \hat{T} - $\hat{\rho}$ phase diagram: L^\pm lines vs coexistence curve; supercritical diameter $\rho_d^> = \frac{1}{2}(\rho^+ + \rho^-)$ vs subcritical diameter $\rho_d = \frac{1}{2}(\rho_L + \rho_G)$. The lines are drawn based on the NIST data.

It has been suggested that the asymmetric effects in the behavior of the subcritical diameter ρ_d originate from the linear mixing of these fields: the coefficients D_1 and D_2 in Eq. (2) depend on a_3, b_2 and $\tan \varphi$ in Eq. (4) [31].

The above setting provides a convenient theoretical model to compute EOSs near the critical point, such as those for the order parameter $\rho(P, T)$ and response function $\kappa_T(P, T)$. Based on these EOSs, we can obtain the supercritical boundary lines L^\pm following the procedure proposed in Ref. [19] (see Appendix A). The idea is to locate the maxima of response functions along lines in parallel to the reference line (i.e., the critical isochore $\rho = \rho_c$ line). Along L^\pm lines, P and ρ follow universal scalings when $\Delta\hat{T} \rightarrow 0$ [19–23],

$$\begin{aligned} \delta\hat{P}^\pm &= A_P^\pm \Delta\hat{T}^\Delta, \\ \delta\hat{\rho}^\pm &= A_\rho^\pm \Delta\hat{T}^\beta, \end{aligned} \quad (5)$$

where $\Delta = \beta + \gamma$ is the gap exponent. Here $\delta\hat{\rho}^\pm$ (and $\delta\hat{P}^\pm$) quantifies the difference between ρ (and P) on the L^\pm lines and that on the critical isochore line (see Fig. 1b). Note that $\delta\hat{\rho}^\pm = \Delta\hat{\rho}^\pm$.

While the scalings in Eq. (5) have been well established in various transitions in liquid-gas [19], liquid-liquid [22], quantum [20, 21], and black-hole systems [22, 23], they are only valid to the lowest order. In order to reveal the asymmetric effects, we need to include higher-order scaling corrections [32]. Specifically, we find that A_P^\pm and A_ρ^\pm in Eq. (5) should include additional T -dependent

terms (see SM Sec. S1),

$$\begin{aligned} A_P^\pm(\Delta\hat{T}) &= A_P^{0,\pm} + A_P^{1,\pm} \Delta\hat{T}^{\Delta-1} + A_P^{2,\pm} \Delta\hat{T}^{1-\alpha} + \dots, \\ A_\rho^\pm(\Delta\hat{T}) &= A_\rho^{0,\pm} + A_\rho^{1,\pm} \Delta\hat{T}^\beta + A_\rho^{2,\pm} \Delta\hat{T}^{\Delta-1} + \dots \end{aligned} \quad (6)$$

For the 3D Ising universality class, $\beta \approx 0.33$, $\Delta-1 \approx 0.56$ and $1-\alpha \approx 0.89$ [33, 34]. The coefficients satisfy,

$$\begin{aligned} A_P^{0,+}/A_P^{0,-} &= -1, & A_P^{1,+}/A_P^{1,-} &= 1, & A_P^{2,+}/A_P^{2,-} &= -1, \\ A_\rho^{0,+}/A_\rho^{0,-} &= -1, & A_\rho^{1,+}/A_\rho^{1,-} &= 1, & A_\rho^{2,+}/A_\rho^{2,-} &= 1. \end{aligned} \quad (7)$$

Very interestingly, the coefficients of some correction terms are “antisymmetric”, with a ratio one. These terms are the origin of asymmetric effects, because they will appear in the scaling of the mean (diameter) of L^\pm lines. In contrast, in the Ising model, $A_P^{n,+}/A_P^{n,-} = A_\rho^{n,+}/A_\rho^{n,-} = -1$ for any order n , and thus all scaling terms cancel in the expression of the diameter.

According to the definitions, $P_d^> = \frac{1}{2}(P^+ + P^-)$ and $\rho_d^> = \frac{1}{2}(\rho^+ + \rho^-)$, Eqs. (5-7) give (with higher-order terms neglected),

$$\begin{aligned} P_d^> &= P_c + d_P |\Delta\hat{T}|^{2\Delta-1}, \\ \rho_d^> &= \rho_c + d_\rho |\Delta\hat{T}|^{2\beta} + e_\rho |\Delta\hat{T}|^{1-\alpha}, \end{aligned} \quad (8)$$

where $d_P = (A_P^{1,+} + A_P^{1,-})/2$, $d_\rho = (A_\rho^{1,+} + A_\rho^{1,-})/2$ and $e_\rho = (A_\rho^{2,+} + A_\rho^{2,-})/2$. Note that the pressure part does not have a subcritical counterpart, because the coexistence region shrinks into a single coexistence line in the P - T phase diagram (see Fig. 1b). The second correction term does not appear in the pressure scaling because of the antisymmetric coefficients, $A_P^{2,+}/A_P^{2,-} = -1$.

In order to test the predictions by experimental data, it is useful to combine Eqs. (5) and (6), and rewrite them using $|\delta\hat{P}|$ as the independent (control) parameter:

$$\begin{aligned} \frac{\Delta\hat{T}^-}{\Delta\hat{T}^+} &= 1 + k_P |\delta\hat{P}|^{1-\frac{1}{\Delta}}, \\ \frac{\delta\hat{\rho}^-}{\delta\hat{\rho}^+} &= 1 + k_\rho |\delta\hat{P}|^{\frac{\beta}{\Delta}} + m_\rho |\delta\hat{P}|^{1-\frac{1}{\Delta}}, \end{aligned} \quad (9)$$

where $\beta/\Delta \approx 0.21$, $1 - \frac{1}{\Delta} \approx 0.36$ and $\frac{1-\alpha}{\Delta} = 0.57$ for the 3D Ising universality class. It suggests that, for the same given $|\delta\hat{P}|$, the ratio of the values of $\Delta\hat{T}$ and $\delta\hat{\rho}$ on the L^\pm lines should follow Eq. (9).

The coefficients $d_P, d_\rho, e_\rho, k_P, k_\rho$ and m_ρ in Eqs. (8) and (9) depend on the mixing coefficients a_3, b_2 and $\tan \varphi$ in Eq. (4) (their expressions are complicated but can be given explicitly; see SM Sec. S1) Importantly, setting $a_3 = b_2 = \tan \varphi = 0$ causes all of these coefficients to vanish. Thus, all asymmetric correction terms come from linear mixing, and are absent in symmetric systems where $h_1 = \Delta\hat{\mu}$ and $h_2 = \Delta\hat{T}$ (such as the lattice gas model). Correspondingly, without linear mixing, the supercritical diameter is rectilinear $\rho_d^> \propto |\Delta\hat{T}|$, a contribution from the non-singular, background part of the thermodynamic potential.

The above results, Eqs. (6-9), are obtained based on complete scaling, i.e., linear mixing of three fields, Eq. (4). If two fields are mixed, e.g., $h_1 = -\tan\varphi\Delta\hat{T} + \Delta\hat{P}$ and $h_2 = \Delta\hat{T} + \tan\varphi\Delta\hat{P}$ [35], then only one asymmetric correction term survives in each expression (see SM Sec. S1 for details).

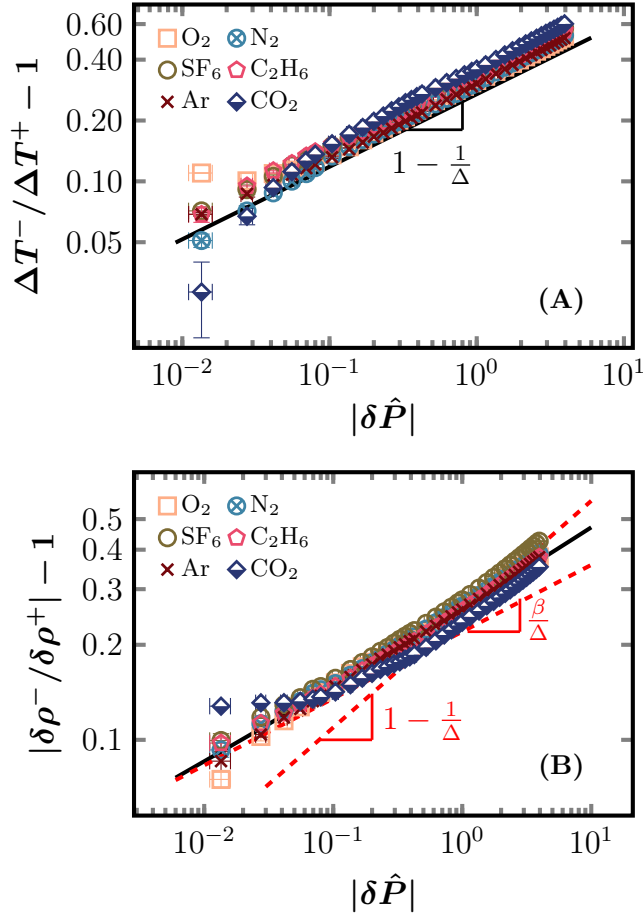


FIG. 3. **Asymmetric effects in supercritical fluids.** The black solid lines are obtained from fitting: (A) $y = 0.27x^{0.36}$; (B) $y = 0.191x^{0.21} + 0.07x^{0.36}$. The red dashed lines in (B) represent the two terms in Eq. (9).

Examination with data of liquid-gas and liquid-liquid phase transitions. To test the above theoretical predictions, we analyze the NIST data of liquid-gas transitions in the following systems [25]: oxygen (O_2), nitrogen (N_2), sulfur hexafluoride (SF_6), ethane (C_2H_6), argon (Ar) and carbon dioxide (CO_2). We will examine Eq. (9), which is practically convenient for an accurate analysis of the data because the L^\pm lines are defined along constant- $\delta\hat{P}$ lines. It should be emphasized that Eq. (9) is mathematically equivalent to the more conventional forms Eqs. (6) and (8).

The L^\pm lines for the above systems are obtained, and the ratios, $\Delta\hat{T}^-/\Delta\hat{T}^+$ and $\delta\hat{\rho}^-/\delta\hat{\rho}^+$, at the same $\delta\hat{P}$, are plotted in Fig. 3. Interestingly, the data nearly collapse. Fitting the data to Eq. (9), with the known 3D Ising

exponents, gives, $k_P = 0.27$, $k_\rho = 0.191$ and $m_\rho = 0.07$. The NIST data show remarkable agreement with our theoretical prediction: the pressure scaling (Fig. 3A) only needs one correction term because only $A_P^{1,\pm}$ are antisymmetric; in contrast, the density scaling (Fig. 3B) requires two correction terms because both $A_\rho^{1,\pm}$ and $A_\rho^{2,\pm}$ are antisymmetric (see Eq. 7).

Our results suggest that all coefficients in Eqs. (8) and (9) are universal for the six systems included in Fig. 3, in contrast to the subcritical case with system-dependent D_1 and D_2 [13]. However, we do find deviation from this universal behavior for the NIST data of hydrogen H_2 (see Appendix B). In general, the subcritical scaling regime of asymmetric corrections appears to be smaller than the supercritical scaling regime. For instance, using the NIST data within the same temperature range $|\Delta\hat{T}| \in [0.001, 0.3]$ as in Fig. 3, we find that the subcritical diameter ρ_d closely follows the rectilinear law, Eq. (2) (see Appendix C). In other words, the violation of the rectilinear diameter law and therefore the asymmetric effects are more difficult to observe below the critical point.

To examine the universality of the asymmetric scaling, we additionally verify Eq. (9) by a mean-field two-state theoretical model of the liquid-liquid phase transition [36, 37]. The model uses mean-field exponents ($\beta = 1/2, \gamma = 1, \alpha = 0$), with other model parameters obtained in [36, 37] by fitting the theoretical EOSs to the experimental data of supercooled water (see Appendix D for details). We find that only first-order corrections are needed, $\frac{\Delta\hat{T}^-}{\Delta\hat{T}^+} = 1 + k_P|\delta\hat{P}|^{1/3}$, and $\frac{\delta\hat{\rho}^-}{\delta\hat{\rho}^+} = 1 + k_\rho|\delta\hat{P}|^{1/3}$. Note that $\beta/\Delta = 1 - 1/\Delta = 1/3$ for the mean-field model.

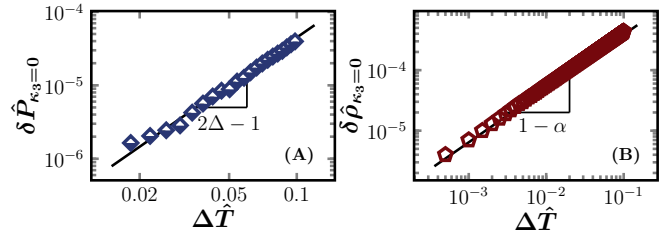


FIG. 4. **Asymmetric effects for the “symmetry line” with $\kappa_3 = 0$.**

Asymmetry revealed by higher-order cumulants of the order parameter distribution. Research interest is developing on understanding the nature of the supercritical state above the conjectured critical point in the quantum chromodynamics (QCD) phase diagram [38–42], for which experimental exploration relies on the measurement of higher-order moments of fluctuating observables, such as the net-proton multiplicity [43–45]. It motivates us to investigate the asymmetric effects in higher cumulants of the order parameter distribution, in the supercritical regime.

Below we consider the EOSs given by a linear scaling theory with parameters $a = k = 0.1$ and $\varphi = 30^\circ$, using 3D Ising universality exponents. To be more explicit, we

mix two fields and therefore only one asymmetric correction term appears in Eq. (8) ($d_\rho = 0$). The n -th cumulants κ_n of the number distribution in a grand canonical ensemble are computed using the formulas provided by the fluctuation solution theory [46, 47] (see SM Sec. S2).

The curve with a zero skewness $\kappa_3 \equiv \langle(N - \langle N \rangle)^3\rangle/V = 0$ is called a “symmetry line” in Ref. [47] for the following reason: the sign of κ_3 indicates favor of particle insertion (in a gas-like state) or removal (in a liquid-like state), and thus a zero κ_3 should correspond to the particle-hole symmetry. However, as shown in Fig. 4, careful examination of the $\kappa_3 = 0$ “symmetry line” shows that it in fact follows the asymmetric scaling, $P_{\kappa_3=0} - P_c \sim |\Delta\hat{T}|^{2\Delta-1}$ and $\rho_{\kappa_3=0} - \rho_c \sim |\Delta\hat{T}|^{1-\alpha}$, as in Eq. (8). Thus, even at the loci where the highest symmetry was suggested, the effects of asymmetry nevertheless endure as an intrinsic property. In addition, these universal scalings also appear in the lines defined by the maxima of κ_4 (see SM

Sec. S2).

Discussion. The supercritical-subcritical correspondence could inspire many future research directions. For instance, it would be interesting to compute a supercritical analog of the latent heat defined by L^\pm lines, and examine its relation to the anomalous phenomenon of supercritical pseudo-boiling [48–50]. The asymmetric effects can be further discussed near the critical points in black hole models [22, 51, 52], QCD systems [38], and quantum magnetic materials [53, 54].

Acknowledgments. Y. J. acknowledges funding from National Key R&D Program of China (Grant No. 2025YFF0512000), Wenzhou Institute (No. WIUCA-SICTP2022) and the National Natural Science Foundation of China (No. 12447101). X. L. acknowledges the Postdoctoral Fellowship Program of CPSF (Grant Number GZC20252776). We acknowledge the use of the High Performance Cluster at Institute of Theoretical Physics, Chinese Academy of Sciences.

-
- [1] M. E. Fisher, Scaling, universality and renormalization group theory, in *Critical Phenomena*, edited by F. J. W. Hahne (Springer Berlin Heidelberg, Berlin, Heidelberg, 1983) pp. 1–139.
- [2] T.-D. Lee and C.-N. Yang, Statistical theory of equations of state and phase transitions. ii. lattice gas and ising model, *Physical Review* **87**, 410 (1952).
- [3] N. Mermin, Lattice gas with short-range pair interactions and a singular coexistence-curve diameter, *Physical Review Letters* **26**, 957 (1971).
- [4] L. Cailletet and E. Mathias, Recherches sur les densités des gaz liquéfiés et de leurs vapeurs saturées, *J. Phys. Theor. Appl.* **5**, 549 (1886).
- [5] S. Reif-Acherman, The history of the rectilinear diameter law, *Quimica nova* **33**, 2003 (2010).
- [6] J. Rehr and N. Mermin, Revised scaling equation of state at the liquid-vapor critical point, *Physical Review A* **8**, 472 (1973).
- [7] N. Wilding and A. Bruce, Density fluctuations and field mixing in the critical fluid, *Journal of Physics: Condensed Matter* **4**, 3087 (1992).
- [8] N. Mermin and J. Rehr, Generality of the singular diameter of the liquid-vapor coexistence curve, *Physical Review Letters* **26**, 1155 (1971).
- [9] B. Widom and J. S. Rowlinson, New model for the study of liquid–vapor phase transitions, *The Journal of Chemical Physics* **52**, 1670 (1970).
- [10] P. Hemmer and G. Stell, Fluids with several phase transitions, *Physical Review Letters* **24**, 1284 (1970).
- [11] M. Ley-Koo and M. S. Green, Revised and extended scaling for coexisting densities of s f 6, *Physical Review A* **16**, 2483 (1977).
- [12] J. Nicoll, Critical phenomena of fluids: asymmetric landau-ginzburg-wilson model, *Physical Review A* **24**, 2203 (1981).
- [13] M. A. Anisimov and J. Wang, Nature of asymmetry in fluid criticality, *Physical review letters* **97**, 025703 (2006).
- [14] M. Pestak, R. E. Goldstein, M. Chan, J. R. de Bruyn, D. Balzarini, and N. Ashcroft, Three-body interactions, scaling variables, and singular diameters in the coexistence curves of fluids, *Physical Review B* **36**, 599 (1987).
- [15] I. Hahn, M. Weilert, F. Zhong, and M. Barmatz, High-resolution measurements of the coexistence curve very near the 3 he liquid–gas critical point, *Journal of low temperature physics* **137**, 579 (2004).
- [16] R. R. Singh and K. S. Pitzer, Rectilinear diameters and extended corresponding states theory, *The Journal of chemical physics* **92**, 3096 (1990).
- [17] Y. Huang, G. Chen, X. Li, and V. Arp, Density equation for saturated 3he, *International journal of thermophysics* **26**, 729 (2005).
- [18] P. Nowak, R. Kleinrahm, and W. Wagner, Measurement and correlation of the (p, ρ , t) relation of nitrogen. ii. saturated-liquid and saturated-vapour densities and vapour pressures along the entire coexistence curve, *The Journal of Chemical Thermodynamics* **29**, 1157 (1997).
- [19] X. Li and Y. Jin, Thermodynamic crossovers in supercritical fluids, *Proceedings of the National Academy of Sciences* **121**, e2400313121 (2024), <https://www.pnas.org/doi/pdf/10.1073/pnas.2400313121>.
- [20] E. Lv, N. Xi, Y. Jin, and W. Li, Quantum supercritical regime with universal magnetocaloric scaling in ising magnets, *Nature Communications* **16**, 10.1038/s41467-025-65651-w (2025).
- [21] J. Wang, E. Lv, X. Li, Y. Jin, and W. Li, Quantum supercritical crossover with dynamical singularity, *Phys. Rev. B* **112**, 195120 (2025).
- [22] S. Wang, X. Li, Y. Jin, and L. Li, Analogous supercritical crossovers in black holes and water, *arXiv preprint arXiv:2506.10808* (2025).
- [23] H.-M. Cui and Z.-Y. Fan, Emergent ising symmetry and supercritical fluids, *arXiv preprint arXiv:2509.17038* (2025).
- [24] S. Jin, X. Li, X. Fan, M. Baggioli, and Y. Jin, Supercritical fluids as a distinct state of matter characterized by sub-short-range structural order, *arXiv preprint*

- arXiv:2508.07385 (2025).
- [25] Nist chemistry webbook, <http://webbook.nist.gov/chemistry/>.
- [26] B. Widom, The critical point and scaling theory, *Physica* **73**, 107 (1974).
- [27] P. Schofield, Parametric representation of the equation of state near a critical point, *Physical Review Letters* **22**, 606 (1969).
- [28] P. Schofield, J. Litster, and J. T. Ho, Correlation between critical coefficients and critical exponents, *Physical Review Letters* **23**, 1098 (1969).
- [29] M. E. Fisher and G. Orkoulas, The yang-yang anomaly in fluid criticality: experiment and scaling theory, *Physical review letters* **85**, 696 (2000).
- [30] Y. C. Kim, M. E. Fisher, and G. Orkoulas, Asymmetric fluid criticality. i. scaling with pressure mixing, *Physical Review E* **67**, 061506 (2003).
- [31] M. Anisimov, V. Agayan, and P. J. Collings, Nature of the blue-phase-iii–isotropic critical point: an analogy with the liquid-gas transition, *Physical Review E* **57**, 582 (1998).
- [32] F. J. Wegner, The critical state, general aspects, *Phase transitions and critical phenomena* **6**, 7 (1976).
- [33] M. Campostrini, A. Pelissetto, P. Rossi, and E. Vicari, 25th-order high-temperature expansion results for three-dimensional ising-like systems on the simple-cubic lattice, *Phys. Rev. E* **65**, 066127 (2002).
- [34] R. Guida and J. Zinn-Justin, Critical exponents of the n-vector model, *Journal of Physics A: Mathematical and General* **31**, 8103 (1998).
- [35] J. Luo, L. Xu, E. Lascaris, H. E. Stanley, and S. V. Buldyrev, Behavior of the widom line in critical phenomena, *Physical Review Letters* **112**, 135701 (2014).
- [36] C. Bertrand and M. Anisimov, Peculiar thermodynamics of the second critical point in supercooled water, *The Journal of Physical Chemistry B* **115**, 14099 (2011).
- [37] V. Holten and M. A. Anisimov, Entropy-driven liquid-liquid separation in supercooled water, *Scientific Reports* **2**, 713 (2012), arXiv:1207.2101 [physics.chem-ph].
- [38] G. Sordi and A.-M. Tremblay, Introducing the concept of the widom line in the qcd phase diagram, *Physical Review D* **109**, 114020 (2024).
- [39] L. Shahkarami and F. Charmchi, Schwinger effect in dynamical holographic qcd with a supercritical region, arXiv preprint arXiv:2509.20151 (2025).
- [40] M. Hanada and H. Watanabe, Partial deconfinement: a brief overview, *The European Physical Journal Special Topics* **232**, 333 (2023).
- [41] L. Y. Glozman, O. Philipsen, and R. D. Pisarski, Chiral spin symmetry and the qcd phase diagram, *The European Physical Journal A* **58**, 247 (2022).
- [42] Y. Fujimoto, K. Fukushima, Y. Hidaka, and L. McLerran, A new state of matter between the hadronic phase and the quark-gluon plasma?, arXiv preprint arXiv:2506.00237 (2025).
- [43] M. Stephanov, Sign of kurtosis near the qcd critical point, *Physical Review Letters* **107**, 052301 (2011).
- [44] M. Aggarwal, Z. Ahammed, A. Alakhverdyants, I. Alekseev, J. Alford, B. Anderson, D. Arkhipkin, G. Averichev, J. Balewski, L. Barnby, et al., Higher moments of net proton multiplicity distributions at rhic, *Physical review letters* **105**, 022302 (2010).
- [45] X. Luo, Q. Wang, N. Xu, and P. Zhuang, Properties of QCD matter at high baryon density, Vol. 10 (Springer, 2022).
- [46] E. A. Ploetz, G. N. Pallewela, and P. E. Smith, Fluctuation solution theory of pure fluids, *The Journal of Chemical Physics* **146** (2017).
- [47] E. A. Ploetz and P. E. Smith, Gas or liquid? the supercritical behavior of pure fluids, *The Journal of Physical Chemistry B* **123**, 6554 (2019).
- [48] D. Banuti, Crossing the widom-line–supercritical pseudo-boiling, *The Journal of Supercritical Fluids* **98**, 12 (2015).
- [49] X. He, J. Xu, X. Yu, and J. Xie, Distinguishing evaporation-like and boiling-like modes of pseudo-boiling in supercritical pressures, *International Journal of Heat and Mass Transfer* **214**, 124417 (2023).
- [50] Q. Wang, X. Ma, J. Xu, M. Li, and Y. Wang, The three-regime-model for pseudo-boiling in supercritical pressure, *International Journal of Heat and Mass Transfer* **181**, 121875 (2021).
- [51] Z.-Y. Li, X.-R. Chen, B. Wu, and Z.-M. Xu, Thermodynamic supercriticality and complex phase diagram for charged gauss-bonnet ads black holes, arXiv preprint arXiv:2511.10357 (2025).
- [52] R. Li, K. Zhang, J. Yang, R. B. Mann, and J. Wang, Critical slowing down of black hole phase transition and kinetic crossover in supercritical regime, *Physical Review D* **112**, 064004 (2025).
- [53] J. L. Jiménez, S. Crone, E. Fogh, M. E. Zayed, R. Lortz, E. Pomjakushina, K. Conder, A. M. Läuchli, L. Weber, S. Wessel, et al., A quantum magnetic analogue to the critical point of water, *Nature* **592**, 370 (2021).
- [54] J. Wang, H. Li, N. Xi, Y. Gao, Q.-B. Yan, W. Li, and G. Su, Plaquette singlet transition, magnetic barocaloric effect, and spin supersolidity in the shastry-sutherland model, *Physical Review Letters* **131**, 116702 (2023).
- [55] J. Wang and M. A. Anisimov, Nature of vapor-liquid asymmetry in fluid criticality, *Phys. Rev. E* **75**, 051107 (2007).
- [56] M. A. Anisimov and J. Wang, Nature of asymmetry in fluid criticality, *Phys. Rev. Lett.* **97**, 025703 (2006).

End Matter

Appendix A: the definition of L^\pm lines. The L^\pm lines are determined according to the following procedure [19]: (i) define a reference line in the field-temperature phase diagram; (ii) draw a series of paths in parallel to the reference line and find the susceptibility (response of the order parameter to the external field) maximum along each path; (iii) connect the loci of susceptibility maxima in the phase diagram. An example of L^\pm is shown in Fig. 1b (in the P - T phase diagram) and Fig. 2 (in the T - ρ phase diagram). The reference line is essential in the definition of L^\pm . For the Ising model, the choice is trivial – the reference line is the T -axis, which coincides with the coexistence line (see Fig. 1a). For the liquid-gas and other asymmetric systems, a natural choice is the critical isochore, i.e., the line with a constant critical density (order parameter) ρ_c . Under the above definition, $\delta\hat{P}^\pm$ quantifies the distance (P difference) from the reference line to L^\pm at the given T , and $\delta\hat{\rho}^\pm$ quantifies their density difference. Note that we use notations with “ δ ” (e.g., $\delta P = P(\rho, T) - P(\rho_c, T)$) to denote the distance to the critical isochore, and those with “ Δ ” (e.g., $\Delta P = P - P_c$) to denote the distance to the critical point.

Appendix B: asymmetric effects in supercritical hydrogen. Fig. 5 shows that the supercritical hydrogen data obtained from NIST deviate from the behavior of systems listed in Fig. 3.

Appendix C: subcritical diameter of carbon dioxide. Fig. 6 shows that the subcritical diameter $\hat{\rho}_d$ of carbon dioxide follows closely the rectilinear law, Eq. (1) – the asymmetric corrections are nearly unobservable. Note that the data plotted in Fig. (3) (supercritical) and those in Fig. 6 (subcritical) cover approximately the same temperature range $\Delta\hat{T} \in [0.001, 0.3]$.

Appendix D: two-state model for liquid-liquid transitions. The two-state model offers a thermodynamic framework for describing polyamorphic single-component liquids by treating them as a binary mixture of two distinct but interconvertible liquid states, denoted as A and B, with corresponding concentrations $1-x$ and x . The present analysis adopts the mean-field formulation of the two-state model, as detailed in Refs. [36, 37]. The molar Gibbs free energy for this binary mixture is,

$$\frac{G}{k_B T} = \frac{G^A}{k_B T} + x \frac{G^{BA}}{k_B T} + x \ln x + (1-x) \ln(1-x) + \omega x(1-x), \quad (10)$$

where k_B is the Boltzmann constant. The term $x \ln x + (1-x) \ln(1-x)$ corresponds to the ideal entropy of mixing, while $\omega x(1-x)$ represents the excess mixing entropy arising from interactions between the A and B states. The interaction parameter is defined as $\omega = 2 + \omega_0 \Delta P$, where ω_0 is a fitting parameter. The quantity $G^A =$

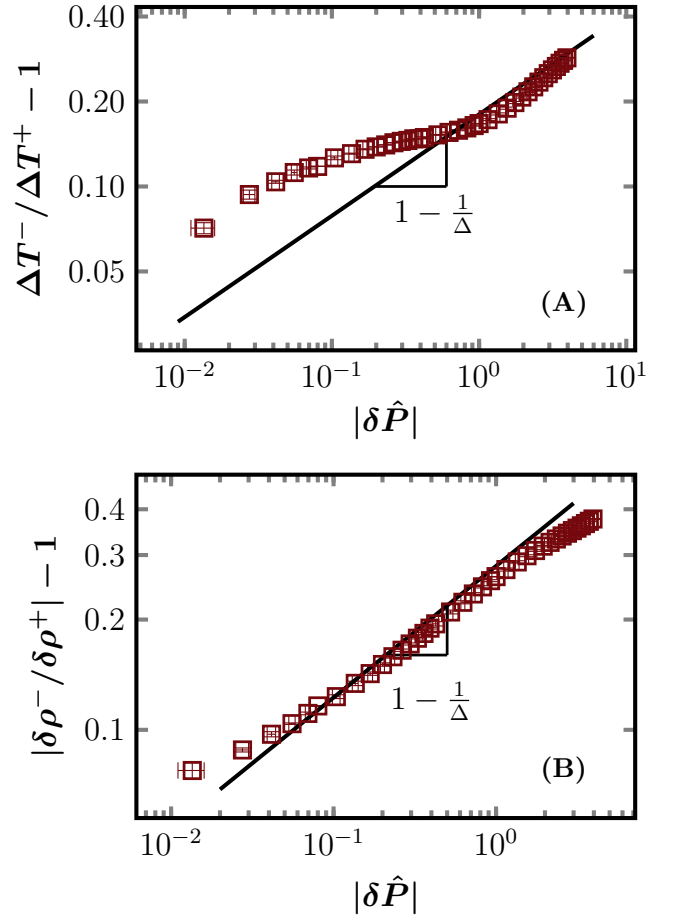


FIG. 5. Asymmetric effects in supercritical hydrogen. The solid fitting line in (A) represents $y = 0.18x^{0.36}$, and the one in (B) represents $y = 0.28x^{0.36}$.

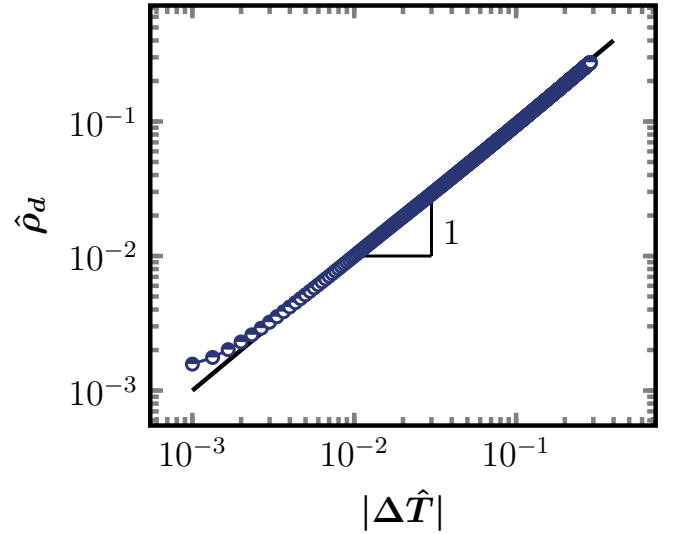


FIG. 6. Asymmetric effects in subcritical carbon dioxide. The solid line is $y = x$.

$\sum_{m,n} c_{mn}(\Delta T)^m(\Delta P)^n$ represents the Gibbs free energy of the pure A state, determined through fitting experimental data with adjustable coefficients c_{mn} . The free energy difference between states B and A is given by $G^{\text{BA}} = G^{\text{B}} - G^{\text{A}}$. In the vicinity of liquid-liquid phase transitions, this difference is approximated by:

$$G^{\text{BA}}/k_{\text{B}}T = \lambda(\Delta T + \alpha_1\Delta P + \alpha_2\Delta T\Delta P), \quad (11)$$

where λ , α_1 , and α_2 are additional fitting parameters. The condition $G^{\text{BA}} = 0$ defines the coexistence line, with parameters α_1 and α_2 characterizing its slope and curvature, respectively.

The equilibrium fraction x is obtained by solving:

$$\mu^{\text{BA}} = G^{\text{BA}} + k_{\text{B}}T \left[\ln \frac{x}{1-x} + \omega(1-2x) \right] = 0, \quad (12)$$

where $\mu^{\text{BA}} = \left(\frac{\partial G}{\partial x} \right)_{T,P}$. The solution of x is then substituted into Eq. (10). The critical parameters T_c , ρ_c , and P_c are also fitting variables. This model exhibits critical scaling behavior consistent with mean-field exponents. Based on these expressions, EOSs can be derived. For instance, the reduced density and reduced volume are given by:

$$\frac{1}{\hat{\rho}(\hat{P}, \hat{T})} = \hat{V}(\hat{P}, \hat{T}) = \left(\frac{\partial \hat{G}}{\partial \hat{P}} \right)_{\hat{T}},$$

employing Eq. (10).

The EOSs of this model are fitted to experimental data of supercooled water in Ref. [37], spanning temperatures from 140 K to 310 K and pressures from 0.1 MPa to 400 MPa. The optimal fit yields critical parameters $T_c = 227.42$ K, $P_c = 13.45$ MPa. Additional fitting parameters are provided in [37]. Note that we choose these fitting parameters to make the model concrete. The scaling behavior is independent of these fitting parameters.

The L^{\pm} loci are identified by determining the maxima of the isothermal compressibility $\kappa_T = \frac{1}{\rho} \left(\frac{\partial \rho}{\partial P} \right)_T$ following the procedure described in Appendix A. Fig. 7 shows the obtained results. Similar to liquid-gas transitions, the data can be fitted to Eq. (9). Because $\beta/\Delta = 1 - 1/\Delta = 1/3$ in the mean-field model, the two correction terms for the density part have the same exponents.

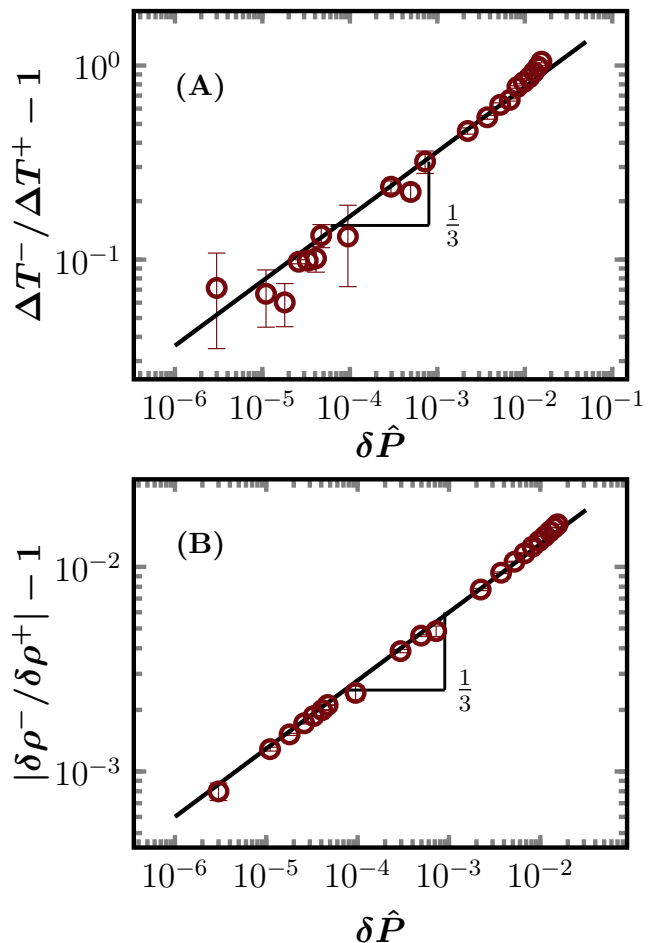


FIG. 7. Asymmetric effects in L^{\pm} lines examined by the two-state model of the liquid-liquid phase transitions. Data are consistent with Eq. (9) with mean-field exponents.

Supplementary Material

CONTENTS

References	5
S1. Scaling theory	9
A. Linear scaling theory	9
B. Linear mixing of three fields	10
C. Symmetric and antisymmetric corrections	12
D. Linear mixing of two fields	12
S2. higher-order cumulants of the particle number distribution.	12

S1. SCALING THEORY

A. Linear scaling theory

The linear scaling theory [27, 28] parameterizes the two external fields h_1 (ordering field) and h_2 (thermal field) with “polar” variables r and θ ,

$$\begin{aligned} h_1 &= ar^{\beta+\gamma}\theta(1-\theta^2), \\ h_2 &= r(1-b^2\theta^2), \end{aligned} \quad (\text{S1})$$

where β and δ are standard critical exponents, a is a system-dependent fitting parameter, and b is a universal parameter obeying $b^2 = (\delta-3)/(\delta-1)(1-2\beta)$. The variable r represents a “distance” from the critical point, and $\theta \in [-1, 1]$ represents the “angle” from the coexistence line ($\theta = \pm 1$). The critical part of thermodynamic potential of a system near the critical point is a homogeneous function of h_1 and h_2 ,

$$h_3 = |h_2|^{2-\alpha} f\left(h_1/|h_2|^{\beta+\gamma}\right), \quad (\text{S2})$$

parameterized as

$$h_3 = r^{2-\alpha} p(\theta), \quad (\text{S3})$$

where $p(\theta)$ is an analytical function. The differential form of h_3 is given by:

$$dh_3 = \phi_1 dh_1 + \phi_2 dh_2. \quad (\text{S4})$$

The order parameter conjugated to h_1 is,

$$\phi_1 = \left(\frac{\partial h_3}{\partial h_1}\right)_{h_2} = r^\beta m(\theta) = kr^\beta \theta, \quad (\text{S5})$$

where $m(\theta)$ is assumed to be a linear function of θ , $m(\theta) = k\theta$ [27, 28], and k is another system-dependent

fitting parameter. The thermodynamic parameter (entropy) conjugated to h_2 is,

$$\phi_2 = \left(\frac{\partial \Psi}{\partial h_2}\right)_{h_1} = r^{1-\alpha} s(\theta). \quad (\text{S6})$$

The function $s(\theta)$ can be determined from the equality

$$\begin{aligned} \left(\frac{\partial \phi_1}{\partial h_2}\right)_{h_1} &= \left(\frac{\partial \phi_2}{\partial h_1}\right)_{h_2}, \\ s(\theta) &= ak(s_0 + s_2\theta^2), \end{aligned} \quad (\text{S7})$$

where,

$$\begin{aligned} s_0 &= -\frac{\beta[-3 + \delta + b^2(-1 + \delta)(-2 + \beta + \beta\delta)]}{2b^4(-2 + \beta + \beta\delta)(-1 + \beta + \beta\delta)}, \\ s_2 &= \frac{\beta(\delta - 3)}{2b^2(-2 + \beta + \beta\delta)}. \end{aligned} \quad (\text{S8})$$

The susceptibilities can be computed using the following expressions,

$$\begin{aligned} \chi_1 &\equiv \left(\frac{\partial \phi_1}{\partial h_1}\right)_{h_2} = \frac{k}{a} r^{-\gamma} C_1(\theta), \\ \chi_2 &\equiv \left(\frac{\partial \phi_2}{\partial h_2}\right)_{h_1} = r^{-\alpha} C_2(\theta), \\ \chi_{12} &\equiv \left(\frac{\partial \phi_1}{\partial h_2}\right)_{h_1} = \left(\frac{\partial \phi_2}{\partial h_1}\right)_{h_2} = kr^{\beta-1} C_{12}(\theta), \end{aligned} \quad (\text{S9})$$

where

$$\begin{aligned} C_1(\theta) &= \frac{(1 - b^2\theta^2(1 - 2\beta))}{C_0(\theta)}, \\ C_2(\theta) &= \frac{[(1 - \alpha)(1 - 3\theta^2)s(\theta) - 2s_2\beta\delta\theta^2(1 - \theta^2)]}{C_0(\theta)}, \\ C_{12}(\theta) &= \frac{\beta\theta[1 - \delta - \theta^2(3 - \delta)]}{C_0(\theta)}, \\ C_0(\theta) &= (1 - 3\theta^2)(1 - b^2\theta^2) + 2\beta\delta b^2\theta^2(1 - \theta^2). \end{aligned} \quad (\text{S10})$$

In a symmetric model such as the lattice-gas model, h_1 and h_2 are related to the physical fields through,

$$\begin{aligned} h_1 &= \Delta\hat{\mu} = (\mu - \mu_c)/k_B T_c, \\ h_2 &= \Delta\hat{T} = (T - T_c)/T_c. \end{aligned} \quad (\text{S11})$$

The corresponding order parameters are $\phi_1 = \Delta\hat{\rho}$ (density change) and $\phi_2 = \Delta(\hat{\rho}\hat{S})$ (entropy density change). The quantity $-h_3$ represents the critical part of the grand thermodynamic potential ($\Omega = -PV$) per unit volume, given by:

$$h_3 = (P - P_{\text{coex}})/(\rho_c k_B T_c), \quad (\text{S12})$$

where P_{coex} denotes the vapor-liquid coexistence pressure, corresponding to the thermodynamic condition $h_1 = 0$.

B. Linear mixing of three fields

To incorporate asymmetry, the scaling fields in the linear scaling theory are expressed as linear combinations of the three physical external fields [29, 30, 55, 56]:

$$\begin{aligned} h_1 &= a_1 \Delta \hat{\mu} + a_2 \Delta \hat{T} + a_3 \Delta \hat{P}, \\ h_2 &= b_1 \Delta \hat{T} + b_2 \Delta \hat{\mu} + b_3 \Delta \hat{P}, \\ h_3 &= c_1 \Delta \hat{P} + c_2 \Delta \hat{\mu} + c_3 \Delta \hat{T}, \end{aligned} \quad (\text{S13})$$

where $\Delta \hat{P} = (P - P_c)/(\rho_c k_B T_c)$. A simplification in defining the coefficients arises from the fact that any two independent critical amplitudes can be included in the homogeneous function $f(x)$ in Eq. (S2); it is therefore convenient to set $a_1 = 1$, $b_1 = 1$ and $c_1 = 1$. Along the coexistence curve and its supercritical extension, defined by $h_1 = 0$, the chemical potential difference $\Delta \hat{\mu}$ vanishes. Thus, the coupling coefficient between $\Delta \hat{P}$ and $\Delta \hat{T}$ is naturally given by the slope of the coexistence curve, $\tan \varphi$, where φ is the slope of the coexistence line. Besides, according to the thermodynamic relation

$$dP = \rho d\mu + \rho S dT, \quad (\text{S14})$$

the critical entropy density is consequently given by $\hat{\rho}_c \hat{S}_c = \left(\frac{\partial \hat{P}}{\partial T}\right)_{h_1=0,c} = \tan \varphi$. Then we can rewrite Eq. (S13) by setting $c_2 = -\rho_c = -1$ and $c_3 = -\rho_c S_c = -\tan \varphi$:

$$\begin{aligned} h_1 &= \Delta \hat{\mu} - a_3 \tan \varphi \Delta \hat{T} + a_3 \Delta \hat{P}, \\ h_2 &= \Delta \hat{T} + b_2 \Delta \hat{\mu} + \tan \varphi \Delta \hat{P}, \\ h_3 &= \Delta \hat{P} - \Delta \hat{\mu} - \tan \varphi \Delta \hat{T}. \end{aligned} \quad (\text{S15})$$

Inverting the expressions gives the physical external fields,

$$\begin{aligned} \Delta \hat{\mu} &= \frac{A_1}{K} h_1 + \frac{B_1}{K} h_2 + \frac{C_1}{K} h_3, \\ \Delta \hat{T} &= \frac{A_2}{K} h_1 + \frac{B_2}{K} h_2 + \frac{C_2}{K} h_3, \\ \Delta \hat{P} &= \frac{A_3}{K} h_1 + \frac{B_3}{K} h_2 + \frac{C_3}{K} h_3, \end{aligned} \quad (\text{S16})$$

where

$$\begin{aligned} A_1 &= b_1 c_1 - b_3 c_3, \\ B_1 &= -a_2 c_1 + a_3 c_3, \\ C_1 &= a_2 b_3 - a_3 b_1, \end{aligned} \quad (\text{S17})$$

$$\begin{aligned} A_2 &= -b_2 c_1 + b_3 c_2, \\ B_2 &= a_1 c_1 - a_3 c_2, \\ C_2 &= -a_1 b_3 + a_3 b_2, \end{aligned} \quad (\text{S18})$$

$$\begin{aligned} A_3 &= b_2 c_3 - b_1 c_2, \\ B_3 &= -a_1 c_3 + a_2 c_2, \\ C_3 &= a_1 b_1 - a_2 b_2, \end{aligned} \quad (\text{S19})$$

and $K = a_1(b_1 c_1 - b_3 c_3) - a_2(b_2 c_1 - b_3 c_2) + a_3(b_2 c_3 - b_1 c_2)$.

Combining Eqs. (S4), (S14) and (S15), we obtain the expressions for the order parameters as follows:

$$\begin{aligned} \hat{\rho} &= \left(\frac{\partial \hat{P}}{\partial \hat{\mu}}\right)_{\hat{T}} = \frac{1 + \phi_1 + b_2 \phi_2}{1 - a_3 \phi_1 - \tan \varphi \phi_2}, \\ \hat{\rho} \hat{S} &= \left(\frac{\partial \hat{P}}{\partial \hat{T}}\right)_{\hat{\mu}} = \frac{\hat{\rho}_c \hat{S}_c - a_3 \tan \varphi \phi_1 + \phi_2}{1 - a_3 \phi_1 - \tan \varphi \phi_2}. \end{aligned} \quad (\text{S20})$$

Performing a Taylor expansion of Eq. (S20) and truncating beyond the linear term in the scaling variable r leads to the following approximation:

$$\begin{aligned} \Delta \hat{\rho} &\simeq (1 + a_3) \phi_1 + a_3 (1 + a_3) \phi_1^2 + (b_2 + \tan \varphi) \phi_2 \\ &\simeq r^\beta [(1 + a_3) k \theta + a_3 (1 + a_3) k^2 r^\beta \theta^2 \\ &\quad + (b_2 + \tan \varphi) r^{\beta+\gamma-1} s(\theta)]. \end{aligned} \quad (\text{S21})$$

The susceptibility is

$$\begin{aligned} \hat{\kappa}_T &= (\partial \hat{\rho} / \partial \hat{\mu})_{\hat{T}} \\ &= (1 + a_3) \left(1 + \frac{2a_3}{1 + a_3} \phi_1\right) \chi_1 \\ &\quad + \left[b_2 + \tan \varphi + b_2 (1 + a_3) \left(1 + \frac{2a_3}{1 + a_3} \phi_1\right)\right] \chi_{12} \\ &\quad + b_2 (b_2 + \tan \varphi) \chi_2. \end{aligned} \quad (\text{S22})$$

From Eq. (S1), we know $r = \left(\frac{h_1}{a\theta(1-\theta^2)}\right)^{\frac{1}{\beta+\gamma}}$. Substituting this relationship and Eqs. (S5) and (S9) into the expression above yields:

$$\begin{aligned} \hat{\kappa}_T(h_1, \theta) &= h_1^{-\frac{\gamma}{\beta+\gamma}} \left\{ A + B h_1^{\frac{\beta}{\beta+\gamma}} + C h_1^{\frac{\beta+\gamma-1}{\beta+\gamma}} \right. \\ &\quad \left. + D h_1^{\frac{2\beta+\gamma-1}{\beta+\gamma}} + E h_1^{\frac{\gamma-\alpha}{\beta+\gamma}} \right\}, \end{aligned} \quad (\text{S23})$$

where

$$\begin{aligned} A &= \frac{k(1+a_3)}{a} C_1(\theta) \cdot (a\theta(1-\theta^2))^{\frac{\gamma}{\beta+\gamma}} \\ B &= \frac{2a_3 k^2}{a} \theta C_1(\theta) \cdot (a\theta(1-\theta^2))^{\frac{\gamma-\beta}{\beta+\gamma}} \\ C &= (\tan \varphi + 2b_2 + a_3 b_2) k C_{12}(\theta) \cdot (a\theta(1-\theta^2))^{\frac{1-\beta}{\beta+\gamma}} \\ D &= 2a_3 b_2 k^2 \theta C_{12}(\theta) \cdot (a\theta(1-\theta^2))^{\frac{1-2\beta}{\beta+\gamma}} \\ E &= b_2 (b_2 + \tan \varphi) C_2(\theta) \cdot (a\theta(1-\theta^2))^{\frac{\alpha}{\beta+\gamma}}. \end{aligned} \quad (\text{S24})$$

Next, we show that θ is a constant along the L^\pm lines. In fact, the quantity $\delta \hat{P}$ is equivalent to h_1 since fixing their values corresponds to paths parallel to the critical isochore. When all the higher-order terms are neglected, the solution that satisfies $\partial \hat{\kappa}_T / \partial \theta = 0$ is found to be independent of h_1 . Consequently, the extremum of $\hat{\kappa}_T$ on such a path, which we define as L^\pm , corresponds to a

constant value of θ . If we substitute $r = \left(\frac{\delta\hat{P}}{a\theta(1-\theta^2)}\right)^{\frac{1}{\beta+\gamma}}$ into Eq. (S16) and (S21), L^\pm lines satisfy

$$\begin{aligned}\Delta\hat{T} &= \frac{A_2}{K}\delta\hat{P} + \frac{B_2}{K}\left(\frac{\delta\hat{P}}{a\theta^\pm(1-\theta^{\pm 2})}\right)^{\frac{1}{\beta+\gamma}}(1-b^2\theta^{\pm 2}) \\ &+ \frac{C_2}{K}\left(\frac{\delta\hat{P}}{a\theta^\pm(1-\theta^{\pm 2})}\right)^{\frac{2-\alpha}{\beta+\gamma}}p(\theta^\pm) \\ &= \tilde{A}_P\delta\hat{P}^{\frac{1}{\beta+\gamma}},\end{aligned}\quad (\text{S25})$$

and

$$\Delta\hat{\rho} \simeq \tilde{A}_\rho\delta\hat{P}^{\frac{\beta}{\beta+\gamma}}, \quad (\text{S26})$$

where

$$\begin{aligned}\tilde{A}_P &= \tilde{A}_P^{0,\pm} + \tilde{A}_P^{1,\pm}\delta\hat{P}^{\frac{\beta+\gamma-1}{\beta+\gamma}} + \tilde{A}_P^{2,\pm}\delta\hat{P}^{\frac{1-\alpha}{\beta+\gamma}} \\ &= \frac{B_2}{K}(a\theta^\pm(1-\theta^{\pm 2}))^{-\frac{1}{\beta+\gamma}}(1-b^2\theta^{\pm 2}) \\ &+ \frac{A_2}{K}\delta\hat{P}^{\frac{\beta+\gamma-1}{\beta+\gamma}} + \frac{C_2}{K}(a\theta^\pm(1-\theta^{\pm 2}))^{-\frac{2-\alpha}{\beta+\gamma}}\delta\hat{P}^{\frac{1-\alpha}{\beta+\gamma}}p(\theta^\pm),\end{aligned}\quad (\text{S27})$$

and

$$\begin{aligned}\tilde{A}_\rho &= \tilde{A}_\rho^{0,\pm} + \tilde{A}_\rho^{1,\pm}\delta\hat{P}^{\frac{\beta}{\beta+\gamma}} + \tilde{A}_\rho^{2,\pm}\delta\hat{P}^{\frac{\beta+\gamma-1}{\beta+\gamma}} \\ &= (1+a_3)k\theta^\pm(a\theta^\pm(1-\theta^{\pm 2}))^{-\frac{\beta}{\beta+\gamma}} \\ &+ a_3(1+a_3)k^2\theta^{\pm 2}(a\theta^\pm(1-\theta^{\pm 2}))^{-\frac{2\beta}{\beta+\gamma}}\delta\hat{P}^{\frac{\beta}{\beta+\gamma}} \\ &+ (b_2 + \tan\varphi)s(\theta^\pm)(a\theta^\pm(1-\theta^{\pm 2}))^{-\frac{1-\alpha}{\beta+\gamma}}\delta\hat{P}^{\frac{\beta+\gamma-1}{\beta+\gamma}}.\end{aligned}\quad (\text{S28})$$

Based on the above results, we can explicitly give the expressions of all coefficients in Eqs. (6-9) in the main text:

$$\begin{aligned}A_P^{0,\pm} &= (\tilde{A}_P^{0,\pm})^{-\Delta} \\ &= a\theta^\pm(1-\theta^{\pm 2})\left(\frac{B_2}{K}(1-b^2\theta^{\pm 2})\right)^{-\Delta} \\ A_P^{1,\pm} &= -\Delta\tilde{A}_P^{1,\pm}(\tilde{A}_P^{0,\pm})^{-2\Delta} \\ &= -\Delta\frac{A_2}{K}a^2\theta^{\pm 2}(1-\theta^{\pm 2})^2\left(\frac{B_2}{K}(1-b^2\theta^{\pm 2})\right)^{-2\Delta} \\ A_P^{2,\pm} &= -\Delta\tilde{A}_P^{2,\pm}(\tilde{A}_P^{0,\pm})^{-\Delta+\alpha-2} \\ &= -\Delta\frac{C_2}{K}a\theta^\pm(1-\theta^{\pm 2})p(\theta^\pm)\left(\frac{B_2}{K}(1-b^2\theta^{\pm 2})\right)^{\alpha-\Delta-2},\end{aligned}\quad (\text{S29})$$

$$\begin{aligned}A_\rho^{0,\pm} &= \tilde{A}_\rho^{0,\pm}(\tilde{A}_P^{0,\pm})^{-\beta} \\ &= (1+a_3)k\theta^\pm\left(\frac{B_2}{K}\right)^{-\beta}(1-b^2\theta^{\pm 2})^{-\beta} \\ A_\rho^{1,\pm} &= \tilde{A}_\rho^{1,\pm}(\tilde{A}_P^{0,\pm})^{-2\beta} \\ &= a_3(1+a_3)k^2\theta^{\pm 2}\left(\frac{B_2}{K}\right)^{-2\beta}(1-b^2\theta^{\pm 2})^{-2\beta}, \\ A_\rho^{2,\pm} &= \tilde{A}_\rho^{2,\pm}(\tilde{A}_P^{0,\pm})^{\alpha-1}, \\ &= (b_2 + \tan\varphi)s(\theta^\pm)\left(\frac{B_2}{K}\right)^{\alpha-1}(1-b^2\theta^{\pm 2})^{\alpha-1},\end{aligned}\quad (\text{S30})$$

$$\begin{aligned}d_P &= \frac{1}{2}(A_P^{1,+} + A_P^{1,-}) \\ &= -\frac{\Delta A_2 a^2}{2K} \\ &\times \sum_{\sigma=\pm}(\theta^\sigma)^2(1-(\theta^\sigma)^2)^2\left(\frac{B_2}{K}(1-b^2(\theta^\sigma)^2)\right)^{-2\Delta},\end{aligned}$$

$$\begin{aligned}d_\rho &= \frac{1}{2}(A_\rho^{1,+} + A_\rho^{1,-}) \\ &= \frac{a_3(1+a_3)k^2}{2}\left(\frac{B_2}{K}\right)^{-\beta}\end{aligned}\quad (\text{S31})$$

$$\begin{aligned}&\times \sum_{\sigma=\pm}(\theta^\sigma)^2(a\theta^\sigma(1-(\theta^\sigma)^2))^{-\frac{\beta}{\Delta}}(1-b^2(\theta^\sigma)^2)^{-\beta}, \\ e_\rho &= \frac{1}{2}(A_\rho^{2,+} + A_\rho^{2,-}) \\ &= \frac{b_2 + \tan\phi}{2}\left(\frac{B_2}{K}\right)^{-\beta} \\ &\times \sum_{\sigma=\pm}s(\theta^\sigma)(a\theta^\sigma(1-(\theta^\sigma)^2))^{\frac{\alpha+\beta-1}{\Delta}}(1-b^2(\theta^\sigma)^2)^{-\beta},\end{aligned}$$

$$\begin{aligned}k_P &= \tilde{A}_P^{1,-}/\tilde{A}_P^{0,-} - \tilde{A}_P^{1,+}/\tilde{A}_P^{0,+} \\ &= \frac{A_2}{B_2}\left[\frac{(a\theta^- (1-\theta^{-2}))^{\frac{1}{\beta+\gamma}}}{1-b^2\theta^{-2}} - \frac{(a\theta^+ (1-\theta^{+2}))^{\frac{1}{\beta+\gamma}}}{1-b^2\theta^{+2}}\right],\end{aligned}\quad (\text{S32})$$

D. Linear mixing of two fields

$$\begin{aligned}
k_\rho &= \tilde{A}_\rho^{1,-}/\tilde{A}_\rho^{0,-} - \tilde{A}_\rho^{1,+}/\tilde{A}_\rho^{0,+} \\
&= a_3 k \theta^- (a\theta^- (1 - \theta^{-2}))^{-\frac{\beta}{\beta+\gamma}} \\
&\quad - a_3 k \theta^+ (a\theta^+ (1 - \theta^{+2}))^{-\frac{\beta}{\beta+\gamma}}, \\
m_\rho &= \tilde{A}_\rho^{2,-}/\tilde{A}_\rho^{0,-} - \tilde{A}_\rho^{2,+}/\tilde{A}_\rho^{0,+} \\
&= \frac{(b_2 + \tan \varphi) s(\theta^-)}{(1 + a_3) k \theta^-} (a\theta^- (1 - \theta^{-2}))^{\frac{\alpha+\beta-1}{\beta+\gamma}} \\
&\quad - \frac{(b_2 + \tan \varphi) s(\theta^+)}{(1 + a_3) k \theta^+} (a\theta^+ (1 - \theta^{+2}))^{\frac{\alpha+\beta-1}{\beta+\gamma}}.
\end{aligned} \tag{S33}$$

C. Symmetric and antisymmetric corrections

Now let us consider the symmetry of the terms in the following expansion:

$$\begin{aligned}
A_P^\pm(\Delta\hat{T}) &= a_P^\pm \left(1 + b_P^\pm \Delta\hat{T}^{\Delta-1} + c_P^\pm \Delta\hat{T}^{1-\alpha} + \dots \right) \\
&= A_P^{0,\pm} + A_P^{1,\pm} \Delta\hat{T}^{\Delta-1} + A_P^{2,\pm} \Delta\hat{T}^{1-\alpha} + \dots,
\end{aligned} \tag{S34}$$

and

$$\begin{aligned}
A_\rho^\pm(\Delta\hat{T}) &= a_\rho^\pm \left(1 + b_\rho^\pm \Delta\hat{T}^\beta + c_\rho^\pm \Delta\hat{T}^{\Delta-1} + \dots \right) \\
&= A_\rho^{0,\pm} + A_\rho^{1,\pm} \Delta\hat{T}^\beta + A_\rho^{2,\pm} \Delta\hat{T}^{\Delta-1} + \dots.
\end{aligned} \tag{S35}$$

Based on the symmetric consideration, we should have $\theta^+ = -\theta^-$. This gives,

(i) asymmetric systems:

$$\begin{aligned}
A_P^{0,+}/A_P^{0,-} &= -1, & A_P^{1,+}/A_P^{1,-} &= 1, & A_P^{2,+}/A_P^{2,-} &= -1, \\
A_\rho^{0,+}/A_\rho^{0,-} &= -1, & A_\rho^{1,+}/A_\rho^{1,-} &= 1, & A_\rho^{2,+}/A_\rho^{2,-} &= 1,
\end{aligned} \tag{S36}$$

where we have used the properties that $p(\theta)$ and $s(\theta)$ are even functions [36]. For symmetric systems like the Ising model, naturally all terms obey the Z_2 symmetry,

(ii) symmetric systems:

$$\begin{aligned}
A_P^{0,+}/A_P^{0,-} &= -1, & A_P^{1,+}/A_P^{1,-} &= -1, & A_P^{2,+}/A_P^{2,-} &= -1, \\
A_\rho^{0,+}/A_\rho^{0,-} &= -1, & A_\rho^{1,+}/A_\rho^{1,-} &= -1, & A_\rho^{2,+}/A_\rho^{2,-} &= -1.
\end{aligned} \tag{S37}$$

Thus, even though according to the Wegner expansion [32], scaling corrections should generically appear in symmetric systems, the “+” and “-” terms strictly cancel each other for the mean (diameter) of L^\pm lines. In contrast, the correction terms can survive in asymmetric systems due to “antisymmetry” (such as $A_P^{1,+}/A_P^{1,-} = 1$). The above analysis reveals that the antisymmetric scaling corrections are the origin of asymmetric effects near the critical point.

The asymmetry arises from two distinct sources: (i) the coupling between two ordering physical fields P and μ , (ii) the inclination ($\tan \varphi$) of the coexistence curve. To see that, let us consider two simpler cases with two-field mixing.

First, if we assume that $b_2 = 0$ and $\tan \varphi = 0$, Eqs. (S15) and (S21) reduce to the following simplified forms:

$$\begin{aligned}
h_1 &= \Delta\hat{\mu} + a_3 \Delta\hat{P}, \\
h_2 &= \Delta\hat{T}, \\
h_3 &= \Delta\hat{P} - \Delta\hat{\mu},
\end{aligned} \tag{S38}$$

and

$$\Delta\hat{\rho} \simeq (1 + a_3)\phi_1 + a_3(1 + a_3)\phi_1^2. \tag{S39}$$

This implies that the coupling between the two ordering fields introduces an asymmetric correction with a critical exponent of 2β since $\phi_1 \sim r^\beta$.

On the other hand, if we simply assume that $a_1 = 0$ and $b_2 = 0$, the forms of these two expressions reduce to:

$$\begin{aligned}
h_1 &= a_3 \tan \varphi \Delta\hat{T} + a_3 \Delta\hat{P}, \\
h_2 &= \Delta\hat{T} + \tan \varphi \Delta\hat{P}, \\
h_3 &= \Delta\hat{P} - \Delta\hat{\mu} - \tan \varphi \Delta\hat{T},
\end{aligned} \tag{S40}$$

and

$$\Delta\hat{\rho} \simeq a_3 \phi_1 + \tan \varphi \phi_2. \tag{S41}$$

This demonstrates that the tilt of the coexistence line introduces an asymmetric correction characterized by the critical exponent $1 - \alpha$ since $\phi_2 \sim r^{1-\alpha}$.

Taking the second scenario as an example, we select the critical exponents of the 3D Ising model, set $a_3 = 1$ and $a = k$ to simplify the parameters, and subsequently compute L^\pm . The result arising from the introduced asymmetry under these conditions is:

$$\begin{aligned}
\frac{\Delta\hat{T}^-}{\Delta\hat{T}^+} &= 1 + k_P |\delta\hat{P}|^{1-\frac{1}{\Delta}}, \\
\frac{\delta\hat{\rho}^-}{\delta\hat{\rho}^+} &= 1 + m_\rho |\delta\hat{P}|^{1-\frac{1}{\Delta}}.
\end{aligned} \tag{S42}$$

As illustrated in Fig. S1, the numerically obtained results agree well with the above expressions.

S2. HIGHER-ORDER CUMULANTS OF THE PARTICLE NUMBER DISTRIBUTION.

We define intensive quantities corresponding to the cumulants κ_n of the number distribution in a grand canonical ensemble, $\kappa_2 = \mu_2/V$, $\kappa_3 = \mu_3/V$ and $\kappa_4 =$

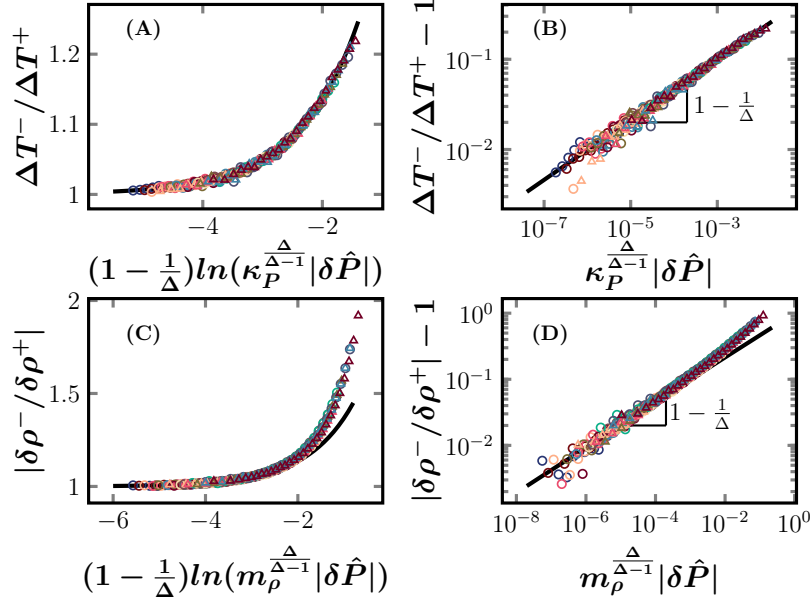


FIG. S1. **Asymmetric effects in L^\pm lines examined by the linear scaling theory.** Data points are obtained from the EOSs given by the linear scaling theory, for $a = 0.1$ ($\phi = 30^\circ, 35^\circ, 40^\circ, 45^\circ, 50^\circ, 55^\circ, 60^\circ, 65^\circ, 70^\circ, 75^\circ, 80^\circ$; circles), and $\phi = 82^\circ$ ($a = 0.02, 0.04, 0.06, 0.08, 0.10$; triangles). The critical exponents are set by the 3D Ising universality class values. The parameters k_P and m_ρ , which depend on a and φ , are obtained by fitting the data to Eq. (S42). The same data plotted in (A,B) semi-log and (C,D) log-log scales. The solid lines are $y = 1 + e^x$ and $y = x^{1-\frac{1}{\Delta}}$.

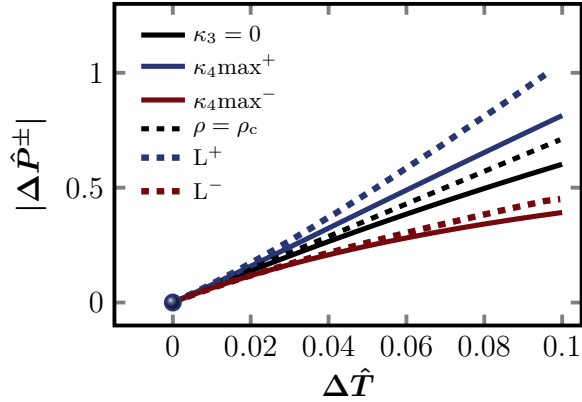


FIG. S2. **Comparison between the $\kappa_3 = 0$, maximum κ_4 lines and critical isochore, L^\pm lines.** Data are obtained from the linear scaling theory with $a = 0.1$ and $\varphi = 82^\circ$.

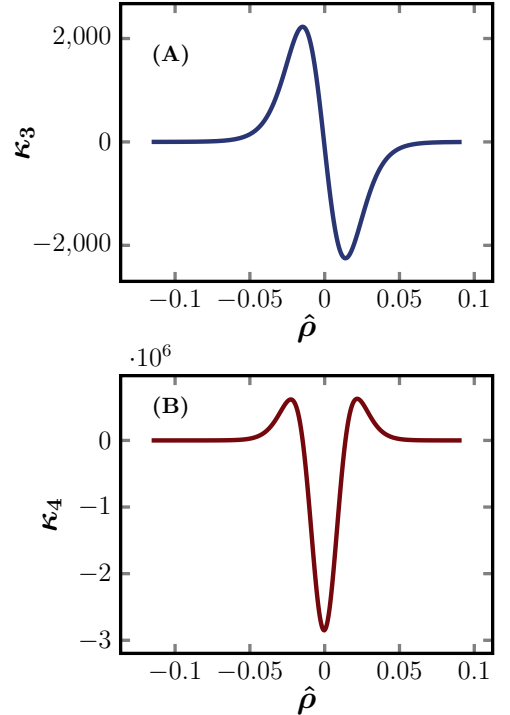


FIG. S3. (A) κ_3 and (B) κ_4 as a function of $\hat{\rho}$ for a chosen T . Data are obtained from the linear scaling theory with $a = 0.1$, $\varphi = 30^\circ$ and $\Delta\hat{T} = 0.1$.

$(\mu_4 - 3\mu_2^2)/V$, where $\mu_n = \langle(N - \langle N \rangle)^n\rangle$ denotes the n -th central moment of particle number fluctuations. The fluctuation solution theory [46, 47] connects κ_n to macroscopic thermodynamic quantities with the following for-

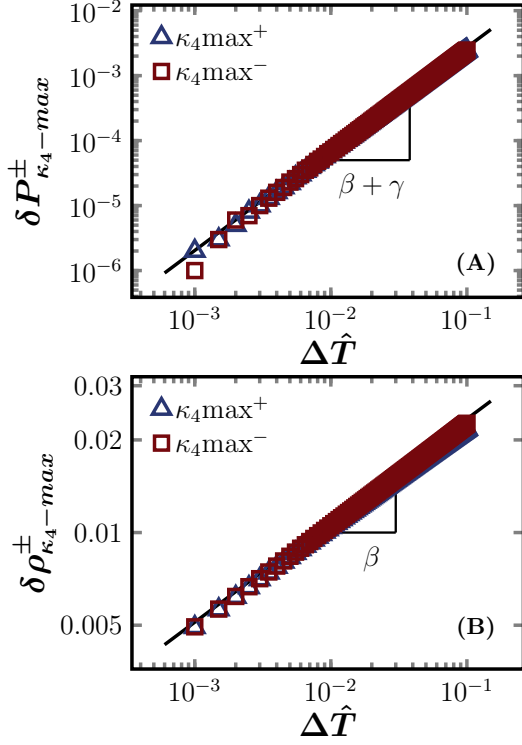


FIG. S4. The (A) pressure and (B) density differences between $\kappa_3 = 0$ and κ_4 -max lines. Data are obtained from the linear scaling theory with $a = 0.1$ and $\varphi = 30^\circ$.

mulas,

$$\begin{aligned}\kappa_3 &= \frac{1}{\beta^2} \left[\rho \left(\frac{\partial \rho}{\partial P} \right)^2 + \rho^2 \left(\frac{\partial^2 \rho}{\partial P^2} \right) \right], \\ \kappa_4 &= \frac{1}{\beta^3} \left[\rho \left(\frac{\partial \rho}{\partial P} \right)^3 - 4\rho^3 \left(\frac{\partial \rho}{\partial P} \right) \left(\frac{\partial^2 \rho}{\partial P^2} \right) + \rho^3 \frac{\partial^3 \rho}{\partial P^3} \right],\end{aligned}\tag{S43}$$

where $\beta = (k_B T)^{-1}$ is the inverse temperature.

The EOSs are given by the linear scaling theory with the simplified two-field linear mixing of physical fields (see Eq. S42). In Fig. S2, the following lines are compared: the L^\pm lines, the $\kappa_3 = 0$ line, and the two lines formed by the loci of κ_4 maxima. Note that $\kappa_4(P)$ or $\kappa_4(\rho)$ has two maxima along an isothermal path [47], see Fig. S3.

It is interesting to examine if the characteristic lines defined by κ_n exhibit the same scalings appearing in L^\pm . We have shown in Fig. 4 that the $\kappa_3 = 0$ line follows the asymmetric scaling Eq. (8). Next we consider the $\kappa_3 = 0$ line as the reference line, and compute the pressure and density differences ($\delta P_{\kappa_4-\max}^\pm$ and $\delta \rho_{\kappa_4-\max}^\pm$) be-

tween the κ_4 -max lines and the reference line, for a given $\Delta \hat{T}$. To the lowest order, these differences satisfy the scalings Eq. (5); see Fig. S4. The next-order correction again shows the expected asymmetric scaling ($k_\rho = 0$ in

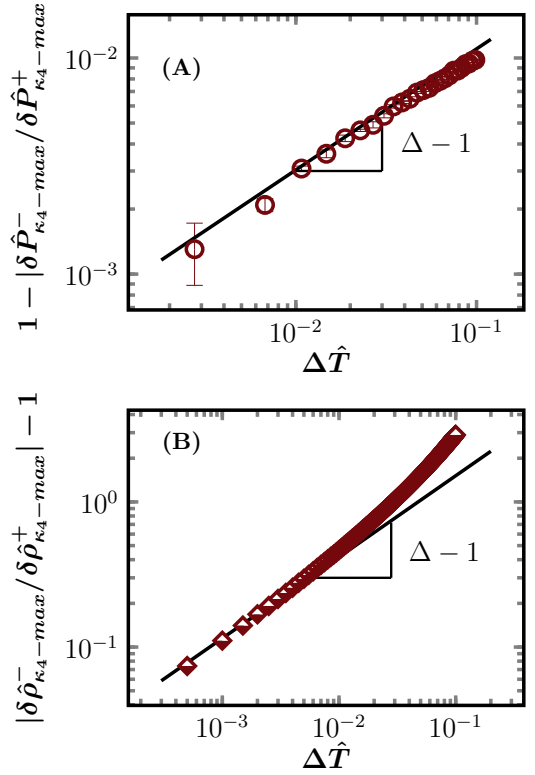


FIG. S5. Asymmetric effects in the two κ_4 -max lines. Data are obtained from the linear scaling theory with $a = 0.1$ and $\varphi = 82^\circ$.

Eq. (9) due to two-field mixing; see Fig. S5).